



Review

Propagative phase shielding solitons in inhomogeneous media

Marcel G. Clerc^a, Mónica A. Garcia-Ñustes^{b,*}, Yair Zárate^a^a Departamento de Física, Facultad de Ciencias Físicas y Matemáticas, Universidad de Chile, Casilla 487-3, Santiago, Chile^b Instituto de Física, Pontificia Universidad Católica de Valparaíso, Avenida Brasil, Valparaíso, Casilla 2950, Chile

HIGHLIGHTS

- We study the propagation of a dissipative soliton in inhomogeneous media.
- Using a solvability condition, an analytical description of soliton dynamics is derived.
- The phase structure self-adjusts and moves rigidly along to the soliton.
- A control mechanism of dissipative solitons is proposed.

ARTICLE INFO

Article history:

Received 21 July 2013

Received in revised form

22 November 2013

Accepted 25 November 2013

Available online 2 December 2013

Communicated by V.M. Perez-Garcia

Keywords:

Dissipative soliton dynamics

Parametrically driven systems

Control mechanism

ABSTRACT

Dissipative solitons in parametrically driven systems propagating in a spatial inhomogeneous medium are investigated. Recently, a family of dissipative solitons with an unexpected shell-type phase structure has been reported. In the present work, we show that the phase configuration moves rigidly along with the modulus after some transient state. Such a transient state is characterized for a self-adaptation of the phase front symmetry and its relative distance to the soliton. The described dynamical behavior is analytically predicted, showing good agreement with numerical simulations. A mechanism of control and manipulation of these structures based on spatial inhomogeneities is proposed.

© 2013 Elsevier B.V. All rights reserved.

1. Introduction

The pioneering works of A. Turing and I. Prigogine [1,2] unveiled that macroscopical systems maintained out of equilibrium, by the injection and dissipation of energy, are self-organizing, showing a wide range of universal phenomena which are independent from the microscopic details of the system under consideration. This capability of self-organization of non-equilibrium systems allows the emergence of dissipative structures such as patterns and localized states [3–5]. The latter are also known as dissipative solitons which can be understood as particle type solutions corresponding to a coherent collective state characterized by a family of continuous parameters like position, width, loading, and so forth [6,7]. Notwithstanding, they are formed by countless constituents. In past decades, these kinds of localized solutions or dissipative solitons have been observed and studied in several non-equilibrium systems including: chain of coupled oscillators,

fluids, optical systems, magnetic and granular media, to mention a few [5–7].

The most efficient way to introduce energy to an oscillatory media is through a resonance phenomenon [8]. Even small periodic driving forces can produce large amplitude oscillations. Among these, the parametrical resonance emerges as a large response of physical systems driven by a temporal modulated parameter. Parametrical resonance is characterized by the exhibition of a subharmonic response [8], i.e. the system is forced at a given frequency and it responds by oscillating to subharmonic frequencies.

A prototype model of a parametrically driven system, which presents dissipative solitons in the quasi-reversal limit—which corresponds to time-reversal systems perturbed with small injection and dissipation of energy [9,10]—is the parametrically-driven and damped nonlinear Schrödinger equation (PDNLS),

$$\partial_t \psi = -i\nu\psi - i|\psi|^2\psi - i\vec{\nabla}^2\psi - \mu\psi + \gamma\bar{\psi}, \quad (1)$$

where $\psi(x, t)$ is a complex field that accounts for the envelope of the oscillation of the system under study. The variable $\bar{\psi}$ stands for the complex conjugate of ψ , and $\{x, t\}$ describe the spatial and temporal coordinates, respectively. ν accounts for the detuning parameter, which is proportional to the difference between half of

* Corresponding author. Tel.: +56 9 98339459.

E-mail addresses: marcel@dfi.uchile.cl (M.G. Clerc), mgarcianustes@ing.uchile.cl, mgarcia16@gmail.com (M.A. Garcia-Ñustes), yair.zarate@ing.uchile.cl (Y. Zárate).

the forcing frequency and the natural frequency of the forced oscillator, μ is the damping parameter which accounts for the energy dissipation processes, and γ is the amplitude of the parametric forcing. Note that the parametrically-driven and damped nonlinear Schrödinger equation (1) is a minimal and universal model. That is, it cannot be further simplified. This model describes an oscillatory focusing media with dispersive coupling [11], since the nonlinear term and spatial coupling have the same sign. Eq. (1) describes qualitatively and quantitatively the system under study in the limit $\nu \sim \mu \sim \gamma \ll 1$. PDNLS has been derived in different physical contexts, such as a vertically oscillating layer of water [12–14], parametrically driven easy-plane ferromagnetic wire [15,16], degenerate optical parametric oscillator [17] and the parametrically driven pendulum chain [18], among others. Model (1) has analytical dissipative solitons with bell-shaped amplitude and homogeneous phase [12,15]. Recently, a novel type of solitons with a shield-type phase structure has been unveiled in parametrically driven systems [19,20]. These types of dissipative solitons have been called *phase shielding solitons*.

A control mechanism of localized structures is the subject of increasing interest due to their technological applications. Several studies have been focused on this problem. Experimental observations of non-propagating hydrodynamic solitons have shown that the water basin inclination can be used as a spatial control tool, since it induces the propagation of dissipative solitons [21,22]. Similarly, recent studies have been performed in the context of semiconductor optical cavities [23], using a phase gradient to induce drifting of cavity solitons. Alternatively, another method of control is through the impurities, since the dissipative solitons are attracted to or repelled by them [18]. However, the phase dynamical behavior has not been considered in most of these works.

The aim of this article is to achieve a characterization of the effects generated by spatial inhomogeneities on dissipative solitons with shield-type phase structure. The inhomogeneities are modeled by means of a spatial variation of the system parameters. As a consequence of these inhomogeneities the dissipative localized state moves rigidly, exhibiting a self-adjustment of the phase front symmetry and the relative distance to the soliton after some transient state. The manuscript is organized as follows: first we review the different dissipative solitons that can be found in the PDNLS model. An adequate analytical description of such localized structures is performed in Section 2. In Section 3 the control mechanism for hydrodynamic solitons proposed in [22] as a manipulation tool for the phase shielding soliton in an inhomogeneous medium is adopted. The soliton modulus speed as a function of a linear spatial variation of the system parameters is analyzed in Section 3.1. Next, introducing a co-moving reference frame, which moves with the soliton position, we could determine the asymptotical front phase speed in Section 3.2. In this co-moving frame, the phase front displays an analogous dynamics such as observed in homogeneous medium. By performing a perturbation analysis, we have determined the characteristic position ξ_{eq} and time τ of the propagative phase shielding soliton. In Section 4, we proposed a possible mechanism of control based on the results obtained. Finally, our conclusions are reported in Section 5.

2. Dissipative solitons in homogeneous medium

The non-propagating hydrodynamics solitons have been observed in a vertically vibrated container with Newtonian fluid [21]. This parametrically forced system is well described by the parametrically-driven and damped nonlinear Schrödinger equation [12,24]. From an ideal fluid assumption, Miles [12] and Larraza and Putterman [24] deduced independently this equation where

the dissipation mechanism has been incorporated phenomenologically. From Eq. (1) one can derive an analytical description for dissipative solitons which are characterized by a bell-like shape in the modulus, and a constant phase [12]. A more detailed treatment of these localized structures with uniform phase and their stability domain can be found in [15] in the context of forced magnetic wires.

2.1. Uniform phase soliton

The uniform-phase soliton solution in parametrically-driven and damped nonlinear Schrödinger equation [12,15] exists in the parameters region bounded by negative detuning ν , and the amplitude of the force between the limiting values $\mu^2 < \gamma^2 < \nu^2 + \mu^2$. In order to obtain an analytical description of the localized states characterized by a uniform phase and a bell-like shape for the amplitude (UPS), we introduce a Madelung transformation, $\psi(x, t) = R(x, t)e^{i\phi(x, t)}$ in Eq. (1),

$$\partial_t R = R\partial_{xx}\phi + 2\partial_x R\partial_x\phi - \mu R + \gamma R \cos(2\phi), \quad (2)$$

$$R\partial_t\phi = -\nu R - R^3 - \partial_{xx}R + R(\partial_x\phi)^2 - \gamma R \sin(2\phi). \quad (3)$$

The nontrivial stationary homoclinic solution in the stationary phase space $\{R, \partial_x R\}$ that connects the quiescent state with itself is given by

$$\cos(2\phi_0) = \frac{\mu}{\gamma}, \quad (4)$$

$$R_s(x) = \sqrt{2\delta_{\pm}} \operatorname{sech} \left[\sqrt{\delta_{\pm}}(x - x_0) \right], \quad (5)$$

where $\delta_{\pm} \equiv -\nu \pm \sqrt{\gamma^2 - \mu^2}$, and x_0 stands for the soliton position. Eq. (4) shows the existence of four phase equilibria ϕ_0 in the interval $[-\pi/2, \pi/2]$, which are relevant in the description of localized states with shield-type phase structure (we shall discuss this later). Notice that only stable uniform-phase solitons can be obtained for δ_+ [15].

2.2. Phase shielding soliton

The first evidence of a complex, non-uniform phase structure in dissipative solitons was provided in the context of soliton interactions [25]. Nevertheless, numerical simulations have shown that even when a single dissipative soliton is perturbed, two unexpected counter-propagative phase fronts arise from the soliton position x_0 , surrounding the bell-shape modulus [19,20] (cf. Fig. 1). The phase front dynamics is characterized by a rather slow motion which suddenly reaches a steady state distant from the soliton position. During this process the shape of both the phase front and the modulus remain unchanged. These novel type of solitons have been called phase shielding solitons (PSS), since the phase structure seems to shield the soliton modulus. Fig. 1 shows the different types of phase shielding solitons. An adequate analytical description of these localized states has been achieved in [19,20]. Next, we briefly review the formalism to describe analytically the general structure and the dynamical behavior of these solutions.

2.2.1. Front phase structure

Different numerical simulations reveal that both phase fronts reach their stationary positions far away and at an equivalent distance each side of the soliton position x_0 (see Fig. 1). Based on these observations, let us introduce the following approximation at a dominate order for the modulus shape,

$$R(x) \approx 2\sqrt{2\delta_+} e^{-\sqrt{\delta_+}(x-x_0)}. \quad (6)$$

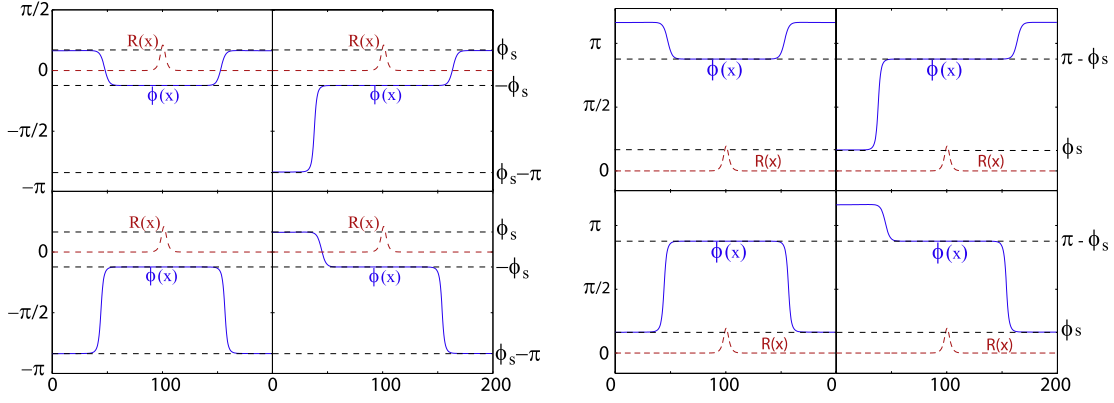


Fig. 1. (Color online) Different phase shielding soliton states in the parametrically driven damped nonlinear Schrödinger equation with $\mu = 0.10$, $\nu = -0.12$, $\gamma = 0.14$, and $L = 200$. Right and left panel: PSS states supported by the inner uniform phase $-\phi_s$ and $\pi - \phi_s$, respectively. Dashed (red) and solid (blue) lines account for the modulus and phase of complex field ψ , respectively.

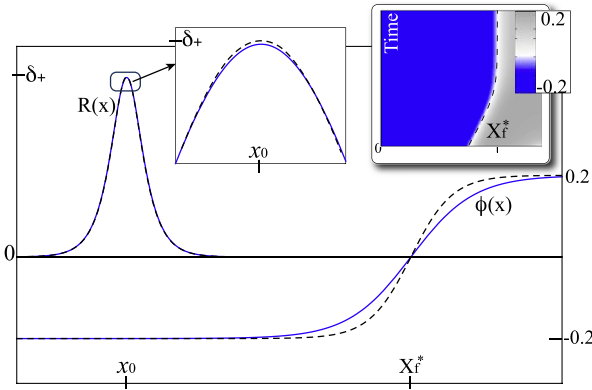


Fig. 2. (Color online) Stationary solution of a typical dissipative soliton with shield-type structure. The inset is the spatiotemporal diagram that shows the front propagation until reach an equilibrium position at X_f^* . The soliton position, X_0 , does not change during this process. The solid and dashed curves account for numerical and analytical solutions, respectively.

Notice that the parameter $\delta_+^{1/2}$ accounts for the exponential decay rate for the modulus of the stable soliton with uniform phase (5). This approximation is valid in the region where $\sqrt{\delta_+} \|x - x_0\| \gg 1$. By replacing the above expression in Eq. (2), one obtains

$$\partial_{xx}\phi = \mu - \gamma \cos(2\phi) + 2\sqrt{\delta_+}\partial_x\phi, \quad (7)$$

which gives us a description of the spatial phase shape. Considering the effective potential $U(\phi) = -\mu\phi + \gamma \sin(2\phi)/2$, Eq. (7) can be understood as a Newton-type equation which describes a particle moving in a tilted periodic potential with an injection of energy proportional to the speed. Equilibrium solutions of model (7) correspond exactly to the uniform phase solutions given by Eq. (4). Indeed, phase fronts connect different uniform phase solutions of Eq. (4) without any observable oscillatory tail (cf. Fig. 2). Hence, the stationary phase front solutions represent heteroclinic orbits in the corresponding stationary dynamical system, $\{\phi, \partial_x\phi\}$ -space, where Eq. (7) can be considered as a Newton-type equation in the overdamped limit.

Introducing the change of variables $x = 2\sqrt{\delta_+}x'$ in Eq. (7), we can perform an asymptotic series $\phi(x) = \varphi_0(x) + \Lambda^1\varphi_1(x) + \Lambda^2\varphi_2(x) + \dots$, with $\Lambda \equiv 1/(4\delta_+) \ll 1$. After straightforward calculations the front phase shape has, at dominant order, the following analytical expression

$$\varphi_F(x, x_f) \approx \varphi_0 = \begin{cases} f_{\text{sol}} - \pi & \text{for } [-\pi, -\pi/2) \\ f_{\text{sol}} & \text{for } (-\pi/2, -\pi/2) \\ f_{\text{sol}} + \pi & \text{for } (\pi, \pi/2] \end{cases} \quad (8)$$

where

$$f_{\text{sol}} = \arctan \left[\sqrt{\frac{\gamma \pm \mu}{\gamma \mp \mu}} \tanh \frac{\sqrt{\gamma^2 - \mu^2}(x - x_f)}{2\sqrt{\delta_+}} \right]. \quad (9)$$

Note that the phase front solutions are also parameterized by the continuous parameter x_f . Considering the complete soliton domain, we obtain the eight possible shell-like configurations that we have previously observed in numerical simulations (see Fig. 1).

Including the first correction in the asymptotic series, the front phase takes the form $\phi^{[1]}(x) = \varphi_0(x) \pm \Lambda\sqrt{\delta_+}\partial_x\varphi_0(x)$. Note that the correction only affects the core region of the front phase, where the phase gradient is not negligible ($\partial_x\varphi_0(x) \neq 0$). The higher corrections have the same implications, but their contributions are negligible. Fig. 2 compares the analytical prediction of Eq. (8) (blue dashed line) with a numerical result (red solid line), exhibiting a good agreement.

2.2.2. Front phase dynamics

As we mentioned above, the phase front propagates through the medium without deforming. Such a dynamics is characterized for being rather slow until it suddenly reaches a steady state far from the soliton position. Therefore, we can consider the phase front position (position where the phase front gradient reaches its maximum) as a time dependent variable $x \equiv X_f(t)$ which accounts for the phase front dynamics. Hence, the phase front takes the form $\phi \equiv \phi(x - X_f(t))$, where $\phi(x)$ is a solution of Eq. (7). Replacing the former ansatz in Eq. (3), we obtain

$$-\dot{X}_f(t)\partial_x\phi = -(\nu + \delta_+) - 8\delta_+e^{-2\sqrt{\delta_+}(x-x_0)} + (\partial_x\phi)^2 - \gamma \sin(2\phi). \quad (10)$$

Multiplying this equation by $\partial_\zeta\phi(\zeta)$, with $\zeta \equiv x - X_f(t)$, and introducing the inner product $\langle f|g \rangle \equiv \int fg dx$. We obtain an equation for the dynamics of the front phase,

$$\dot{X}_f(t) = A + Be^{-2\sqrt{\delta_+}(X_f(t)-x_0)}, \quad (11)$$

where

$$A \equiv \frac{\langle (\nu + \delta_+ + \gamma \sin(2\phi) - (\partial_\zeta\phi)^2) | \partial_\zeta\phi \rangle}{\langle \partial_\zeta\phi | \partial_\zeta\phi \rangle}, \quad (12)$$

and

$$B \equiv 8\delta_+ \frac{\langle e^{-2\sqrt{\delta_+}\zeta} | \partial_\zeta\phi \rangle}{\langle \partial_\zeta\phi | \partial_\zeta\phi \rangle}. \quad (13)$$

These constants are real numbers, which can be either positive or negative depending on the shape of the phase front. For instance,

when one considers a front that increases monotonically with the spatial coordinate, A (B) is a negative (positive) constant.

The equation for the phase front speed, Eq. (11), is characterized by two parts. The term proportional to A that accounts for the constant speed at which the larger phase value invades the smaller one giving rise to a phase front which propagates towards the position of the soliton x_0 . In contrast, the term proportional to B accounts for the effect of spatial variation of the tail of the amplitude soliton, which induces a drift that leads to phase fronts moving away from the position of the soliton. Consequently, the superposition of these two antagonistic forces generates a stable equilibrium for the position of the phase front

$$X_f^* = x_0 - \frac{1}{2\sqrt{\delta_+}} \log\left(-\frac{A}{B}\right), \quad (14)$$

which represents a characteristic length of the phase shielding soliton, since it varies continuously depending on the parameters. Fig. 2 shows the position of the soliton and phase front. The inset illustrates the dynamics of the phase front. The position x_f is reached after some transient state. Recently, phase shielding solitons have been characterized and observed in forced magnetic media [20].

A deeper analysis of numerical simulations reveals that PSS solutions are constituted by two qualitatively different regions: inner and outer regions. The inner and outer regions stand for the central and asymptotic part of the PSS, respectively. These regions are a consequence of a crossover between the exponential tails of UPS solutions. Indeed, the stable and unstable UPS exponential decay rates are proportional to $\sqrt{\delta_+}$ and $\sqrt{\delta_-}$, respectively. Given that $\delta_+ > \delta_-$, the slower unstable decay rate crosses the stable faster one. This effect is almost discernible in the modulus of the soliton but becomes relevant in the phase. The crossover is characterized by a transition point which outlines the border transition between the inner and outer regions and corresponds to the characteristic length of the phase shielding soliton l_f . It is clear from this, that if the system size L is small enough ($L < l_f$), the crossover will not take place and we observe only the usual UPS solution. A more detailed analysis about the inner and outer region and higher order corrections of Eq. (2) can be found in Ref. [20].

3. Phase shielding solitons in an inhomogeneous medium

A systematic analytical and experimental study concerning non-propagating hydrodynamic solitons in a tilted basin has been developed in Ref. [22]. As consequence of the inclination of the channel, the system parameters become inhomogeneous, whose variation depend on the depth of the fluid. Therefore, to account for this phenomenon, one needs to incorporate spatial inhomogeneities in the parameters of the parametrically-driven and damped nonlinear Schrödinger equation. Thus, the parameters of PDNLS take the general form:

$$\begin{aligned} \mu &\rightarrow \mu_0 + \mu_1(x), \\ \gamma &\rightarrow \gamma_0 + \gamma_1(x), \\ \nu &\rightarrow \nu_0 + \nu_1(x) \end{aligned} \quad (15)$$

where $\{\mu_0, \gamma_0, \nu_0\}$ and $\{\mu_1, \gamma_1, \nu_1\}$ account for homogeneous and inhomogeneous spatial variation, respectively. Given that parametrically-driven and damped nonlinear Schrödinger equation is valid in the quasi-reversible limit ($\nu \sim \mu \sim \gamma \ll 1$) we consider the inhomogeneities as perturbative effects, i.e. we set $\mu_1(x) \ll \mu_0$, $\gamma_1(x) \ll \gamma_0$ and $\nu_1(x) \ll \nu_0$. For stability reasons of the soliton solution, $\gamma(x)$ must always satisfy the condition

$$\mu_0 < \gamma(x) \leq \sqrt{\nu_0^2 + \mu_0^2} \text{ in the } \{\nu, \gamma\} \text{ parameter space.}$$

We have carried out numerical simulations of phase shielding solitons in the PDNLS model setting up $\mu_0 = \nu_0 = 0$ and $\gamma(x)$

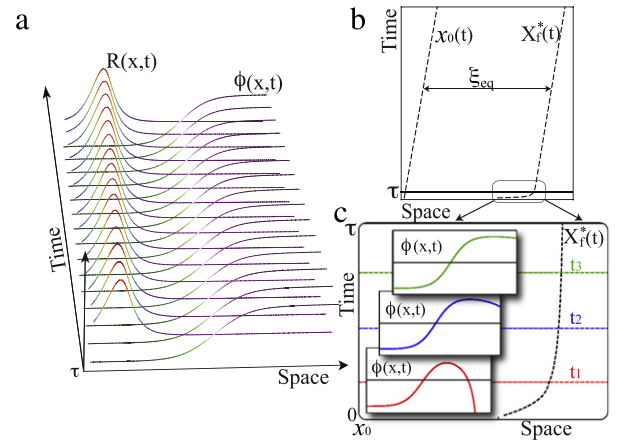


Fig. 3. Phase shielding soliton behavior in an inhomogeneous medium with $\sigma = 0.004$, $\mu = 0.1$, $\gamma = 0.108$, $\nu = -0.05$, and $L = 128$. (a) After the transient state $t > \tau$, the module starts and phase propagates slowly with a constant speed as a rigid solid. (b) Spatiotemporal diagram showing modulus and front positions, respectively. The phase front reaches a new characteristic distance ξ_{eq} in a moving frame aligned with the modulus position $X_c(t)$. (c) Process of self-adaptation of a monotonously increasing phase configuration for $t < \tau$.

is described by a linear ramp or a smooth quadratic function. The algorithm used is a scheme of finite difference for the space (with up to 2 neighbors) with Neumann boundary conditions and a fourth order Runge–Kutta algorithm for the time evolution. Fig. 3 displays the characteristic dynamics of a propagative phase shielding soliton under the effect of a linear ramp for the forcing parameter. As a result of the inhomogeneity, the soliton position starts to drift slowly through the medium, maintaining its bell-like shape (see Fig. 3(a)). The phase front, meanwhile, exhibits a much richer and complex dynamics characterized by a relaxation time, τ (cf. inset Fig. 3). For a time lower than τ ($t < \tau$), the front phase propagates with a rapidly decreasing speed. At $t = \tau$ the front phase reaches a roughly constant speed similar to the soliton position speed. During this period, the front displays an self-adaptive process, where the inner region undergoes a shrinkage of its length, i.e., the characteristic length scale X_f decreases. From there on the propagative phase shielding soliton moves as a rigid solid (cf. Fig. 3).

3.1. Soliton position speed

We start our analysis introducing the following regions: the central and sideways region, which characterize the soliton spatial structure. The central region is defined as the domain around the soliton position where the phase is uniform. The sideways regions are the complementary to the central one (cf. Fig. 4). In the first case, the PSS propagation problem can be reduced to a uniform phase soliton which propagates in a slightly inhomogeneous medium. In Ref. [22], a procedure for a non-propagative hydrodynamic soliton in a tilted basin is proposed, which corresponds to considering a dissipative soliton with a constant phase. Adopting the proposed strategy, we promote the soliton position as a dynamical variable, $x_0 \equiv x_0(t)$. Hence, let us consider the following ansatz,

$$R(x, t) = R_s(x - x_0(t)) + \rho(x, x_0(t)), \quad (16)$$

$$\phi(x, t) = \phi_0 + \Omega(x, x_0(t)), \quad (17)$$

where $\rho(x, x_0(t))$ and $\Omega(x, x_0(t))$ are small corrective functions. The soliton position $x_0(t)$ is a slow variable ($\ddot{x}_0(t) \ll \dot{x}_0(t) \ll 1$), whose speed $\dot{x}_0(t)$ is of the same order of the perturbation. Introducing the above expressions and the inhomogeneous

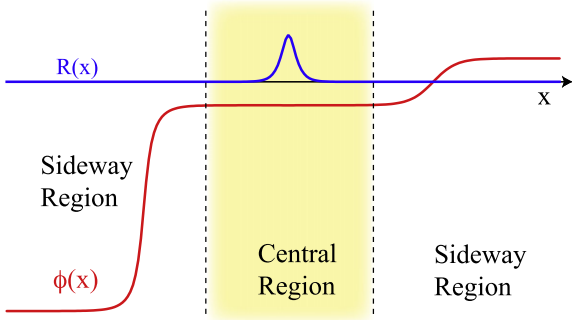


Fig. 4. The domain is divided into two different regions; inner and outer. This separation is maintained during the entire propagation of solitons.

parameters (15) in Eqs. (2) and (3), and linearizing at first order in perturbations, one finds

$$2\partial_x R_s \partial_x \Omega + R_s \partial_{xx} \Omega = 2\gamma_0 \sin(2\phi_0) R_s \Omega + \mu_1(x) R_s - \gamma_1(x) \cos(2\phi_0) R_s - \dot{x}_0 \partial_{\xi} R_s, \quad (18)$$

$$\mathcal{L}\rho = \nu_1(x) R_s + 2\gamma_0 \cos(2\phi_0) R_s \Omega + \gamma_1 \sin(2\phi_0) R_s, \quad (19)$$

where ϕ_0 and R_s are defined by Eqs. (4) and (5), respectively. $\xi(t) \equiv x - x_0(t)$ stands for the coordinate in the co-moving frame. The linear operator defined as $\mathcal{L} \equiv -\nu_0 - \gamma_0 \sin(2\phi_0) - 3R_s^2 - \partial_{xx}$ is a Sturm–Liouville operator. Multiplying the partial differential equation (19) by the integrating factor R_s , it can be rewritten as

$$\begin{aligned} \Omega(x) = & \int^x \frac{2\gamma_0 \sin(2\phi_0) dx'}{R_s^2(x')} \int^{x'} dx'' \Omega(x'') R_s^2(x'') \\ & + \int^x \frac{dx'}{R_s^2(x')} \int^{x'} dx'' [\mu_1(x'') \\ & - \gamma_1(x'') \cos(2\phi_0)] R_s^2(x'') - \int^x \frac{\dot{x}_0}{2} dx', \end{aligned} \quad (20)$$

which is a Fredholm integral equation [26]. In the quasi-reversible limit holds $\gamma_0 \sin(2\phi_0) = \sqrt{\gamma_0^2 - \mu_0^2} \ll 1$. Hence we can consider the following approximation as a solution of the above Eq. (20)

$$\begin{aligned} \Omega(x) \approx & - \int^x \frac{\dot{x}_0}{2} dx' + \int^x \frac{dx'}{R_s^2(x')} \\ & \times \int^{x'} dx'' [\mu_1(x'') - \gamma_1(x'') \cos(2\phi_0)] R_s^2(x''). \end{aligned} \quad (21)$$

Notice that one can iteratively calculate the corrections of the previous approximation in a power series of the small parameter $\sqrt{\gamma_0^2 - \mu_0^2}$ [26].

To achieve a solution for ρ , Eq. (19), we use the Fredholm alternative (see Ref. [4] and references therein). Accordingly, we introduce the inner product

$$\langle f | g \rangle = \int f(x) g(x) dx.$$

Hence, the Sturm–Liouville operator \mathcal{L} is self-adjoint ($\mathcal{L} = \mathcal{L}^\dagger$). The kernel of \mathcal{L} —the set of functions v that satisfy $\mathcal{L}v = 0$ —has dimension 1. As a result of the spatial translation invariance the soliton solution satisfies $\mathcal{L}\partial_x R_s = 0$, which is a consequence of the Goldstone mode. Then, the linear equation (19) has a solution if the following condition is fulfilled (solvability condition),

$$\langle \partial_x R_s | 2\mu_0 R_s \Omega + \gamma_1(x) \sin(2\phi_0) R_s + \nu_1(x) R_s \rangle = 0. \quad (22)$$

Replacing the approach (21) in the above condition, one obtains after straightforward calculations,

$$\begin{aligned} \dot{x}_0 = & \frac{1}{\int_{-\infty}^{\infty} dx x \partial_x R_s^2(x)} \left[2 \int_{-\infty}^{\infty} dx \partial_x R_s^2(x) \int^x \frac{dx'}{R_s^2(x')} \right. \\ & \times \int^{x'} dx'' [\mu_1(x'') - \gamma_1(x'') \cos(2\phi_0)] R_s^2(x'') \\ & \left. + \frac{1}{\mu_0} \int_{-\infty}^{\infty} dx [\gamma_1(x) \sin(2\phi_0) + \nu_1(x)] \partial_x R_s^2(x) \right]. \end{aligned} \quad (23)$$

The above kinetic law allow us to characterize the soliton speed for any slightly inhomogeneous medium. For better understanding we will discuss in the next section the effects produced by a linear inhomogeneous medium.

3.1.1. Linear inhomogeneous medium

For the sake of simplicity, we consider the detuning ν and dissipative parameter μ as homogeneous parameters, $\mu_1(x) = \nu_1(x) = 0$. Meanwhile the forcing amplitude is described by a linear ramp function,

$$\gamma(x) \equiv \gamma_0 + \sigma x, \quad (24)$$

where σ is the inhomogeneity parameter.

By setting the dependency of the parameters according the expression (24), the speed of the modulus takes the simple form

$$\dot{x}_0 = \alpha \sigma, \quad (25)$$

where,

$$\begin{aligned} \alpha \equiv & \frac{\sin(2\phi_0)}{\mu_0} - \frac{2 \cos(\mu_0)}{\int_{-\infty}^{\infty} dx x \partial_x R_s^2(x)} \\ & \times \int_{-\infty}^{\infty} dx \partial_x R_s^2(x) \int^x \frac{dx}{R_s^2(x)} \int^{x'} dx'' x'' R_s^2(x''), \end{aligned} \quad (26)$$

is a real number depending of the system parameters. From Eq. (25), we obtain that the soliton propagates at constant speed proportional to the inhomogeneity coefficient. In Fig. 3(a), we display a numerical simulation of a soliton propagating in a linear inhomogeneous medium described by expression (24). Clearly, the soliton exhibits a constant speed propagation as shown in the spatiotemporal diagram of Fig. 3(b).

3.2. Phase front propagation

In the sideways regions, the uniform phase approach is no longer valid. Notwithstanding the contribution of the modulus, $R(x - x_0(t))$ in this region can be approximated at dominant order by its exponential tail, expression (6), which moves rigidly at speed $\dot{x}_0(t)$ (cf. Fig. 4). This allows us to rewrite the front velocity (11) in a co-moving frame system

$$\dot{X}_f(t) = A + B e^{-2\sqrt{\delta_+}(X_f(t) - x_0)}, \quad (27)$$

with A and B given by formulas (12) and (13), respectively. The above equation accounts for the front phase dynamics in an inhomogeneous medium. Introducing the co-moving coordinate $\xi(t) \equiv X_f(t) - x_0(t)$, the front phase velocity takes the form

$$\dot{\xi}(t) = A - \dot{x}_0(t) + B e^{-2\sqrt{\delta_+}\xi(t)}, \quad (28)$$

where $\dot{x}_0(t)$ is the soliton position speed given by Eq. (23). The above kinematic equation possesses three different components. The first term of the right side accounts for the difference between both phase states, the second and the last term describe the co-moving frame imposed by the soliton position motion and the inhomogeneous variation of the modulus tail, respectively.

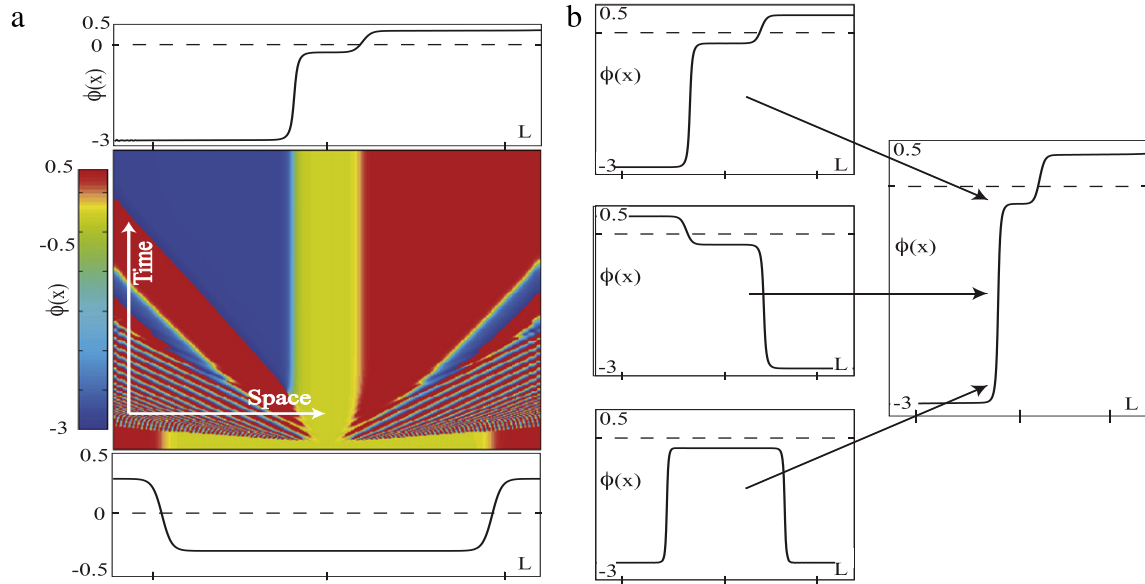


Fig. 5. Four different PSS have been taken as initial conditions in the inhomogeneous medium. (a) Symmetric PSS was taken as initial condition (bottom). Immediately there emerge a transient state followed by an auto-adaptation process. The remaining structure is the asymmetric PSS (top). (b) Regardless of which was the initial condition, the final remaining solution is the asymmetric PSS.

3.2.1. Linear inhomogeneous medium

As we already showed, in the presence of an inhomogeneous medium where there exists a spatial dependency of the parameters according to expression (24), the modulus speed becomes proportional to the coefficient related to the inhomogeneity σ (see Eq. (25)). Therefore, the phase front speed in the co-moving system has the form

$$\dot{\xi}(t) = A - \alpha\sigma + Be^{-2\sqrt{\delta_+}\xi(t)}. \quad (29)$$

Notice that the above equation has the same form of Eq. (11). Therefore, in the co-moving system, the phase front develops the same characteristic dynamics exhibited in a homogeneous medium (see inset Fig. 2). Fig. 3(a) displays the typical dynamical behavior of a phase shielding soliton subject to a linear inhomogeneous forcing $\gamma(x)$ given by expression (24). As seen in Fig. 3(b), at a characteristic time τ , the phase front reaches a constant velocity, remaining at an equilibrium distance ξ_{eq} in the co-moving frame. Therefore, from there on ($t > \tau$) the propagative phase shielding soliton travels as a rigid body. By fixing $\dot{\xi} = 0$, we calculate the equilibrium position ξ_{eq} ,

$$\xi_{\text{eq}} = -\frac{1}{2\sqrt{\delta_+}} \log\left(\frac{c\sigma - A}{B}\right). \quad (30)$$

This equilibrium position stands for the characteristic length of the propagative phase shielding soliton in the co-moving frame (see inset Fig. 3(b)). By considering a perturbation of the form $\xi(t) = \xi_{\text{eq}} + \eta(t)$ with ($\eta(t) \ll 1$) in the velocity expression (29),

$$\dot{\eta} = -2\sqrt{\delta_+}(A - \alpha\sigma)\eta, \quad (31)$$

we get an estimate of the characteristic time

$$\tau \propto 1/\lambda = 1/(2\sqrt{\delta_+}(A - \alpha\sigma)). \quad (32)$$

Performing a perturbation analysis of the form $\Delta(\tau) \equiv z_0 - \zeta(\tau)$ (see Fig. 6), we are able to obtain the dependency of the difference between the front phase equilibrium position as a function of the inhomogeneity parameter σ , which has the analytical expression at dominant order

$$\Delta(\tau) \approx \frac{\alpha\sigma}{2\sqrt{\delta_+}B} e^{2\sqrt{\delta_+}X_f}. \quad (33)$$

Notice that the above difference depends exponentially on the front position in an homogeneous medium (X_f). This implies that the characteristic length of the phase in an inhomogeneous medium is exponentially sensitive to small spatial variations of the forcing amplitude σ . Therefore, corrections over such length are not negligible. This places in evidence that the phase structure is sensitive to disturbances.

For $t < \tau$ the phase dynamics goes through a process of self-adaptation, where the structure itself can drastically change (see Fig. 3(c)). The above analysis only considers variations over the characteristic length of the front position not a structural change of the phase configuration. Hence, this approach is only valid for phase shielding solitons that keep the same phase configuration when they are subject to an inhomogeneous spatial forcing. Numerical simulations reveal that the monotonously increasing phase (asymmetric PSS) configurations holds its shape in an inhomogeneous medium. Therefore, our analysis is valid for this type of configuration. Fig. 5 displays the initial configuration of a typical phase shielding soliton which is subject to a linear spatial inhomogeneous forcing. After a very intricate deformation of the phase ($t < \tau$), the soliton adopts a monotonously increasing phase structure which evolves until reaching its final equilibrium position in the co-moving system. Notwithstanding, the right panel of Fig. 5 shows the initial and final state for three dissimilar phase configurations. All these initial conditions evolve to the same final asymmetric PSS configuration for $t > \tau$. Hence, the analysis is valid for any configuration only considering $t \gg \tau$. For the initial transient of some PSS configurations it is not possible (using the perturbation method as a strategy) to describe the observed dynamics despite the parameter inhomogeneity being a small perturbation.

4. Mechanism of control

The manipulation of localized structures constitutes the basis of most technology applications. Due to these structures are the responsible for storing and transporting information [6,7]. Based on previous results (see Section 3), we propose a mechanism of control that allows us to manage at will the localized solution, either its speed of propagation as well as its position (cf. Fig. 7). Although the time dependence of the ramp slope σ can allow us to control the behavior of the soliton, there are important considerations to make

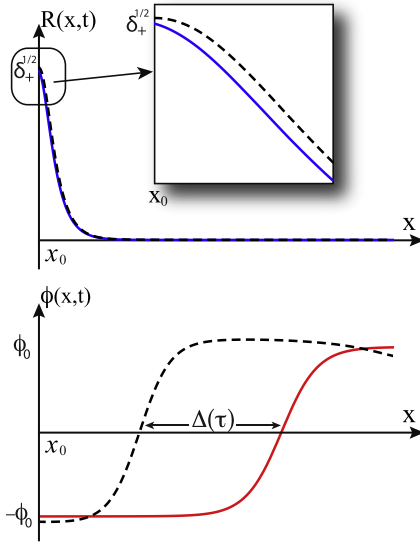


Fig. 6. Figure shows the differences between a PSS propagating in an inhomogeneous medium (dashed black lines) and a steady one. Top: Modulus of both phase shielding solitons. Bottom: For $\sigma > 0$ (24) the front phase of the propagative phase shielding soliton (dashed line) is closer to the modulus core than the homogeneous case (solid line). $\Delta(\tau)$ is defined as the difference between the front equilibrium positions.

just to get a proper management of the structure. In fact, a minimal condition is that $\gamma(x, t)$ takes values in time and space ensuring the stability (or existence) condition $\mu \leq \gamma(x, t) \leq \sqrt{\mu^2 + \nu^2}$. Hence, to guarantee that we are manipulating the soliton through the inhomogeneous medium without wave radiation [25,18], we introduce the following suitable inhomogeneous forcing parameter

$$\gamma(x, t) = \begin{cases} \gamma_0, & t \leq t_1 \\ \gamma_0 + \sigma(x - x_0), & t_1 \leq t \leq t_2 \\ \gamma_0 + \sigma^2 \alpha(t_2 - t_1), & t \geq t_2, \end{cases} \quad (34)$$

where γ_0 , x_0 , α , and σ stand for the initial parameter forcing, the initial soliton position, proportionality constant of the speed defined in expression (26), and the inhomogeneity parameter, respectively. t_1 and t_2 are the initial and final times for which the soliton propagates (cf. Fig. 7). As we can see, the slope of the ramp changes discontinuously (as a step function) in time.

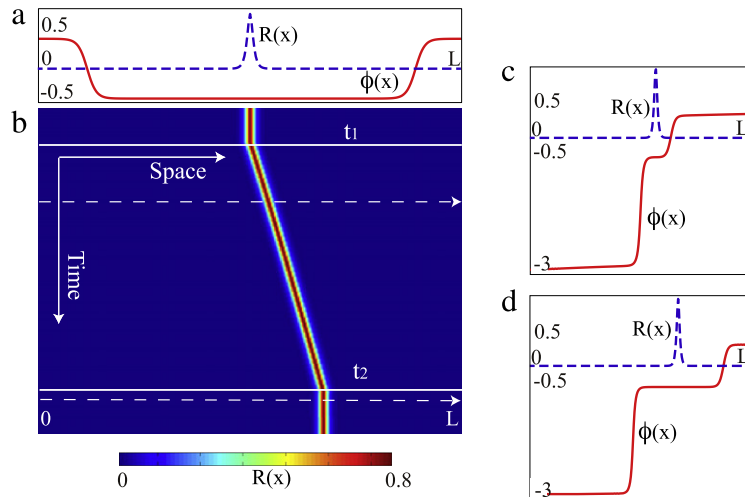


Fig. 7. Control of PSS dynamics by using the linear manipulation mechanism proposed with $\gamma_0 = 0.15$, $\nu = -0.16$, $\mu = 0.1$, and system size $L = 300$. (a) The initial PSS solution before it starts to propagate $\sigma(0) = 0$. (b) Spatiotemporal diagram of the whole soliton dynamics subject to a control mechanism. (c) Profile of the propagative PSS while drifting ($\sigma(t) = 0.00017$). (d) The stationary final PSS solution after removing the inhomogeneity ($\sigma(t) = 0$).

To illustrate this procedure we conducted a numerical simulation of PSS on an inhomogeneous medium. Fig. 7 displays the spatiotemporal dynamics of the modulus of a PSS solution achieved by applying the above control method. In Fig. 7(a) we show the PSS solution before introducing the inhomogeneity ($t < t_1$). At $t = t_1$, the phase shielding soliton starts to propagate through the medium. As seen in Fig. 7(b) the propagative PSS moves at a constant speed as a rigid solid (cf. 7(c)). Finally we remove the inhomogeneous forcing parameter and the soliton stops in its final ($t > t_2$) position. Fig. 7(d) shows the final stationary PSS solution. We want to emphasize the difference in the characteristic length (X_f) between the propagative PSS and the steady one (Fig. 7(c) and (d), respectively) which is consistent with the previous discussion of the effects produced by the inhomogeneities over the phase structure (Section 3.2).

5. Conclusions

We have investigated the propagation of phase shielding solitons in an inhomogeneous medium. In homogeneous media, the modulus of the soliton remains stationary, meanwhile the phase exhibits a front propagation dynamics until reaching an equilibrium position at X_f^* . This position constitutes a characteristic length of the phase shielding soliton.

Following previous works we have studied the soliton dynamics under consideration of spatial variations of the system parameters $\{\mu(x), \nu(x), \gamma(x)\}$. In the particular case, when the soliton is subject to a linear ramp forcing $\gamma(x) \equiv \gamma_0 + \sigma x$ (μ, ν constant) we have shown that the soliton modulus propagates at a constant speed proportional to the inhomogeneity coefficient σ . Notwithstanding, the phase front presents a nontrivial dynamics distinguished by a characteristic time τ . The phase front, seen in a moving frame aligned to the modulus position, displays a dynamical behavior analogous to that predicted in a homogeneous system. That is, the front phase of the soliton moves at nonconstant speed ($t < \tau$), exhibiting a self-adapting process until reaching an equilibrium position $\xi_{eq} < X_f^*$ in the co-moving frame ($t = \tau$). From there on, the propagative phase shielding soliton starts to drift as a rigid body ($t > \tau$). Using a Madelung transformation and a Fredholm alternative, we derived an expression for both the characteristic time τ and the equilibrium position at the co-moving frame ξ_{eq} .

Since the dynamics of the propagative PSS is completely determined by the parameter σ , it can be adopted as a manipulation tool of dissipative solitons. We perform numerical

simulations to show a soliton is moved in a controlled manner. To prevent waves radiation and loss of soliton stability, we manipulate the soliton using a linear step ramp.

Acknowledgments

The authors acknowledge financial support from the ANR-CONICYT 39, “Colors”. M.G.C. and M.A.G.-N. are thankful for the financial support of FONDECYT projects 1120320 and 3110024, respectively. Y.Z. acknowledges the financial support of CONICYT by Beca Magister Nacional.

References

- [1] A.M. Turing, The chemical basis of the morphogenesis, *Phil. Trans. R. Soc. A* 237 (1952) 37–72.
- [2] G. Nicolis, I. Prigogine, *Self-Organization in Non Equilibrium Systems*, Wiley, New York, 1977.
- [3] M. Cross, H. Greenside, *Pattern Formation and Dynamics in Nonequilibrium Systems*, Cambridge University Press, New York, 2009.
- [4] L.M. Pismen, *Patterns and Interfaces in Dissipative Dynamics*, in: Springer Series in Synergetics, Berlin, Heidelberg, 2006.
- [5] M.C. Cross, P.C. Hohenberg, Pattern formation outside of equilibrium, *Rev. Modern Phys.* 65 (1993) 851–1112.
<http://dx.doi.org/10.1103/RevModPhys.65.851>.
URL: <http://link.aps.org/doi/10.1103/RevModPhys.65.851>.
- [6] N. Akhmediev, A. Ankiewicz, *Dissipative Solitons: From optics to Biology and Medicine*, Springer, Berlin, Heidelberg, 2008.
- [7] O. Descalzi, M. Clerc, S. Residori, G. Assanto, *Localized States in Physics: Solitons and Patterns*, Springer, New York, 2011.
- [8] L. Landau, E.M. Lifshitz, *Mechanics*, Pergamon Press, United Kingdom, 1969.
- [9] M. Clerc, P. Couillet, E. Tirapegui, The Maxwell–Bloch description of 1/1 resonances, *Opt. Commun.* 167 (1999) 159–164.
- [10] M. Clerc, P. Couillet, E. Tirapegui, Lorenz bifurcation: instabilities in quasireversible systems, *Phys. Rev. Lett.* 83 (19) (1999) 3820–3823.
- [11] V.I. Arnold, *Geometrical Methods in the Theory of Ordinary Differential Equations*, Springer-Verlag, New York, 1988.
- [12] J. Miles, Parametrically excited solitary waves, *J. Fluid Mech.* 148 (1984) 451–460.
- [13] W. Zhang, J. Vinals, Secondary instabilities and spatiotemporal chaos in parametric surface-waves, *Phys. Rev. Lett.* 74 (5) (1995) 690–693.
- [14] X. Wang, R. Wei, Oscillatory patterns composed of the parametrically excited surface-wave solitons, *Phys. Rev. E* 57 (1998) 2405–2410.
<http://dx.doi.org/10.1103/PhysRevE.57.2405>.
URL: <http://link.aps.org/doi/10.1103/PhysRevE.57.2405>.
- [15] I. Barashenkov, M. Bogdan, V. Korobov, Stability diagram of the phase-locked solitons in the parametrically driven, damped nonlinear Schrödinger equation, *Europhys. Lett.* 15 (1991) 113.
- [16] M. Clerc, S. Coulibaly, D. Laroze, Localized states beyond the asymptotic parametrically driven amplitude equation, *Phys. Rev. E* 77 (5) (2008) 056209.
- [17] S. Longhi, Stable multipulse states in a nonlinear dispersive cavity with parametric gain, *Phys. Rev. E* 53 (5) (1996) 5520–5522.
- [18] N. Alexeeva, I. Barashenkov, G. Tsironis, Impurity-induced stabilization of solitons in arrays of parametrically driven nonlinear oscillators, *Phys. Rev. Lett.* 84 (14) (2000) 3053–3056.
- [19] M. Clerc, S. Coulibaly, M.A. Garcia-Ñustes, Y. Zárate, Dissipative localized states with shieldlike phase structure, *Phys. Rev. Lett.* 107 (25) (2011) 254102.
- [20] M. Clerc, S. Coulibaly, M.A. Garcia-Ñustes, Y. Zárate, Phase shielding soliton in parametrically driven systems, *Phys. Rev. E* 87 (25) (2013) 052915.
- [21] J. Wu, R. Keolian, I. Rudnick, Observation of a nonpropagating hydrodynamic soliton, *Phys. Rev. Lett.* 52 (1984) 1421–1424.
- [22] L. Gordillo, T. Sauma, Y. Zárate, I. Espinoza, M.G. Clerc, N. Mujica, Can non-propagating hydrodynamic solitons be forced to move? *Eur. Phys. J. D* 62 (2010) 39–49.
- [23] E. Caboche, F. Pedaci, P. Genevet, S. Barland, M. Giudici, J. Tredicce, G. Tissoni, L.A. Lugiato, Microresonator defects as sources of drifting cavity solitons, *Phys. Rev. Lett.* 102 (2009).
- [24] A. Larraza, S. Putterman, Theory of non-propagating surface-wave solitons, *J. Fluid Mech.* 148 (1984) 443–449.
- [25] I. Barashenkov, E. Zemlyanaya, Stable complexes of parametrically driven, damped nonlinear Schrödinger solitons, *Phys. Rev. Lett.* 83 (13) (1999) 2568–2571.
- [26] G. Arfken, H. Weber, *Mathematical Methods for Physicists*, Elsevier Academic Press, Burlington, 2001.